SPECTROSCOPY OF ρ, ω AND ϕ FAMILIES (FROM PHOTOPRODUCTION AND e^+e^- ANNIHILATION)

E. PAUL
PHYSIKALISCHES INSTITUT
University of Bonn
Bonn, Federal Republic of Germany

ABSTRACT

A review is given of recent results on the vector mesons ρ^0, ω, ϕ, and on radial excitations of these states obtained in photoproduction at high energies and in e^+e^- annihilations. New results on J/ψ photoproduction are also reported.

CONTENTS

1. INTRODUCTION

The main subject of this talk is the recent experimental results on vector mesons anticipated as radial excitations of ρ^0, ω and ϕ. In a popular spectroscopic picture they are considered as $q\bar{q}$ states of the type indicated in fig. 1. Radial excitations are distinguished from ground states by the mass only.
We consider here states built up by the so-called light quarks u, d and s. Candidates for radial excitations of such states have been discussed for a long time. Wellknown candidates of the $\rho(770)$ family are $\rho'(1600)$ and $\rho'(1250)$.

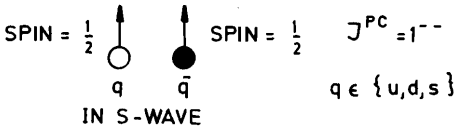

Fig. 1 Quark model for vector mesons

Interest in such old-fashioned vector mesons was reawakened by the discovery of the ψ and T families. There the existence of radial excitations was established and appropriate descriptions in terms of potential models were found. It is interesting to look for the link to the light-quark states. At present no straightforward extrapolation from heavy-quark states to light-quark states exists. Various open questions have still to be answered. For instance, one may ask /1/:

- What are the relevant masses of the light-quarks? Are they dressed as suggested by deep inelastic electron scattering results?
- Do relativistic effects contribute?
- Are light-quarks sensitive to long range components of the potential?

For such questions, experiments on light quark-hadron spectroscopy /2/ are so far not very conclusive, mainly since important landmarks like radial excitations are rarely experimentally settled.

Unique experimental possibilities exist for neutral vector mesons which can couple to the photon. The experiments to explore them utilize preferentially this coupling. Also the radial excitation states should couple to the photon; however, they are expected -for general reasons- to have weaker coupling strengths (fig.2).

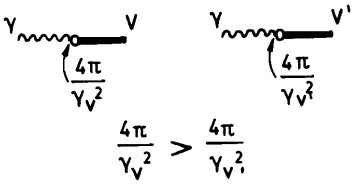

Fig.2 Photon-vector meson couplings

Three types of experiments are established. These are (fig.3):

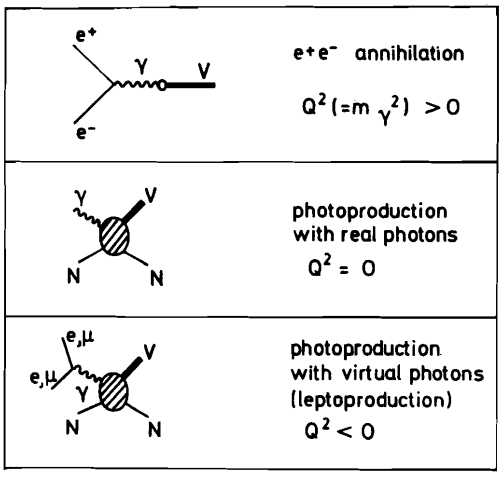

Fig.3 Diagrams for photoinduced vector meson production

e^+e^- annihilations with a virtual massive photon of $Q^2 > 0$, photoproduction with real photons of $Q^2 = 0$, and leptoproduction (virtual photoproduction) with $Q^2 < 0$. A link between these processes is provided by the Vector Meson Dominance (VMD) model which assumes that the photon can be decomposed into vector meson states

$$|\gamma> \;=\; \sum_V \frac{4\pi}{\gamma_V^2}\,|V> \;.$$

For e^+e^- annihilations this implies that the final hadronic states originate from decaying vector mesons with vector meson-photon coupling strengths related to the leptonic partial width by the well-known relation

$$\frac{4\pi}{\gamma_V^2} = \frac{12}{\alpha^2}\,\frac{\Gamma(V\to e^+e^-)}{m_V} \qquad (1)$$

where $\Gamma(V \to e^+e^-)$ is the partial width of the leptonic vector meson decay.

For photoproduction VDM implies in the simplest case that the photon couples to a vector meson and this is then scattered diffractively as indicated by the diagram in fig. 4a. In the approximation that the photoproduction of a vector meson is described by this term only, useful relations are derived:

$$\frac{d\sigma}{dt}(\gamma N \to VN) = \frac{\alpha}{4}\frac{4\pi}{\gamma_V^2}\frac{d\sigma}{dt}(VN \to VN) \qquad (2)$$

and with the optical theorem

$$\frac{d\sigma}{dt}(\gamma N \to VN)\Big|_{t=0} = \frac{\alpha}{64\pi}\frac{4\pi}{\gamma_V^2}\sigma_{TOT}^2(VN).\{1+\eta_V^2\} \qquad (3)$$

where η_V is the ratio of the real to the imaginary part of the forward scattering amplitude. By means of these relations one can extract from the photoproduction cross section the vector meson scattering cross section, if the coupling strength is known (or vice versa). Alternatively, both can be determined simultaneously from measurement on heavy nuclei (in the framework of Glauber multiple scattering theory). In simple VMD it is moreover assumed that this coupling strength is the same in e^+e^- annihilations and in photoproduction so that the production of a vector meson in one process implies predictions for the other according to (1), (2) and (3).

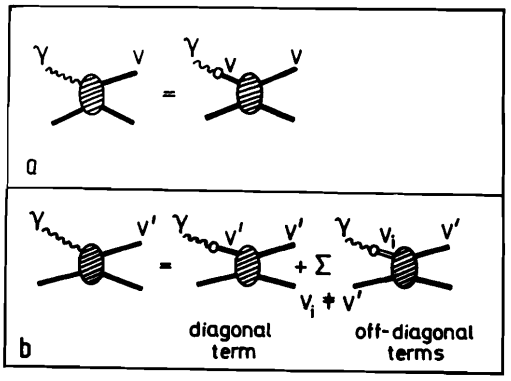

Fig.4 Vector Meson Dominance diagrams illustrating photoproduction of "normal" vector mesons (a) and of radial excitations (b) where the sum is taken over all vector mesons other than V'.

The diagonal assumption is useful when describing the gross features of photoproduction of the ground states ρ^o, ω and ϕ. However, for radial excitations of these states due to the reduced coupling strength, so-called off-diagonal terms have to be taken into account (fig.4b). In particular, the process where the ground state produces a radial excitation state by a diffraction dissociation mechanism is estimated to contribute with a strength similar to that of the diagonal term. (Such an estimate is deduced from the experimentally observed diffraction dissociation processes of hadrons /3/). In this more complex case there is no longer the simple possibility to extract coupling strengths or hadronic cross sections from photoproduction data /4/, and, moreover, the simple comparison with e^+e^- annihilations is somewhat spoiled.

A first check of the VMD hypothesis is obtained from the measurement of the ratio R in e^+e^- annihilations as a function of the energy as shown in fig.5. Below 1.1 GeV, where ρ, ω and ϕ dominate, the data support the VMD hypothesis /48/. However,

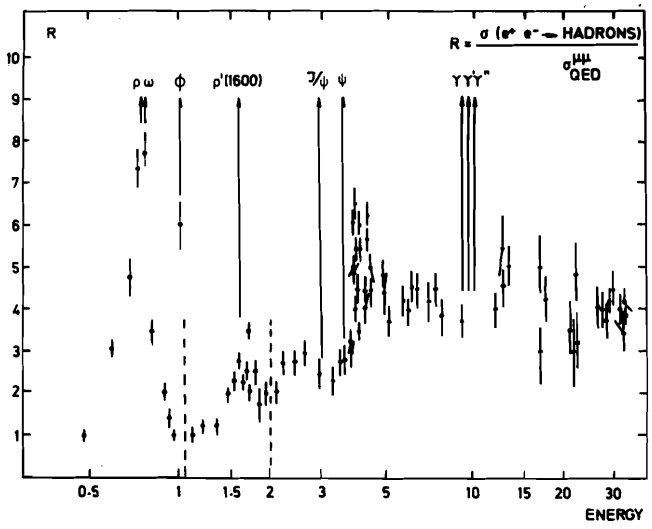

Fig.5 Measurements of the ratio R in e^+e^- annihilations.

the range from 1.1 GeV up to ∿ 2 GeV, predicted to be the domain of radial excitation of ρ, ω and φ, for example in a Veneziano-like spectrum /5/, shows no resonance-like structures except for a broad bump at ∿ 1.6 GeV, suggesting that there is the ρ'(1600). The ratio R does not tell us whether there is indeed a series of resonances (broad and overlapping) or a single broad resonance on top of a continuum. Certainly detailed analyses of exclusive final states are needed.

The current experimental activities connected to this field of physics are summarized in fig.6. Results on e^+e^- annihilations are submitted to this conference from the DM1 spectrometer at the DCI ring at Orsay /6/ and from Novosibirsk (OLYA) /3/. In high energy photoproduction new results are available from the broad band spectrometer at FNAL /7/ and from two experiments with the OMEGA spectrometer at CERN /8, 9, 1o, 11, 12/.

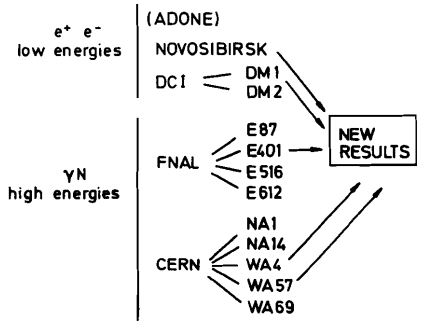

Fig.6 Experimental activities.

2. PHOTOPRODUCTION OF ρ^o, ω, φ AND J/ψ AT HIGH ENERGIES

Recent experiments have extended the photon energy range for ρ^o, ω and φ photoproduction up to 18o GeV /8, 14-16/ and for J/ψ up to 3oo GeV /7/. I select here only few of the new results.

2.1 The shape of the ρ^o in $\gamma p \to \pi^+\pi^- p$

In lower energy experiments it was found that the ρ^o shape observed in photoproduction of $\pi^+\pi^-$ pairs off hydrogen was "skewed" in comparison with a p-wave Breit-Wig-

ner distribution /17/. This skewing effect is now also observed at photon energies from 2o to 7o GeV by the OMEGA-Photon Collaboration at CERN /8/ as shown in fig.7.

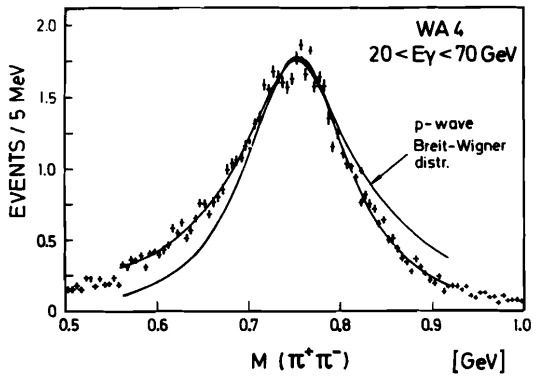

Fig.7 Mass distribution of the $\pi^+\pi^-$ system observed in the reaction $\gamma p \to \pi^+\pi^- p$ /8/.

By quantitative comparisons it was found that there is no obvious difference to lower energies. This means that the main ideas for explaining it, for instance the Söding interference model /18, 19/, appear to be valid.

2.2 Production mechanism of $\gamma p \to \omega p$ at photon energies from 2o to 7o GeV.

In the case of ω photoproduction it was found that unnatural parity exchange (pion exchange) was an important contribution at lower photon energies /17/. With increasing photon energy it is expected that the non-diffractive contributions become relatively small so that there are more similarities between ω and ρ^o photoproduction. In a new experiment (WA57) the OMEGA-Photon Collaboration studied the angular distributions of the ω decay into $\pi^+\pi^-\pi^o$ produced with partially polarized photons which were tagged in the photon energy range from 2o to 7o GeV. The $\pi^+\pi^-\pi^o$ mass distribution shows a clear ω signal (fig. 8). The measured angular distributions for the ω decay are shown in fig. 9. They are consistent with the predictions expected for s-channel helicity conservation (SCHC) and purely natural parity exchange /2o/ (curves in fig. 9). So it was concluded that the data are consistent with there being no contribution from unnatural parity exchange in ω photoproduction unlike the lower energy results.

2.3 Elastic photoproduction of ρ^o, ω and ϕ in comparison to elastic scattering of hadrons

Total cross sections for elastic ρ^o, ω and ϕ photoproduction are shown as a function of the photon energy in fig. 1o. Such distributions were discussed by Eisner at the 1979 Photon-Lepton Conference /21/ and are up-dated here by results at the intermediate photon energy range from 2o to 7o GeV. The data are compared to predictions derived using simple VMD from measurements of pion and kaon elastic

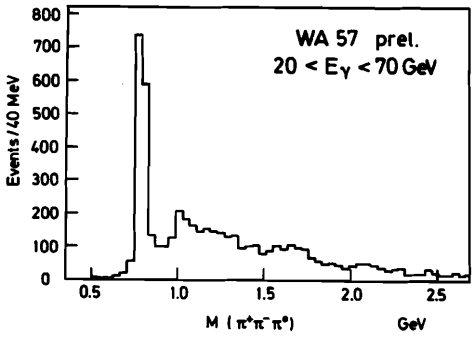

Fig. 8
Mass distribution of the $\pi^+\pi^-\pi^0$ system observed in the reaction $\gamma p \rightarrow \pi^+\pi^-\pi^0 p$ /11/.

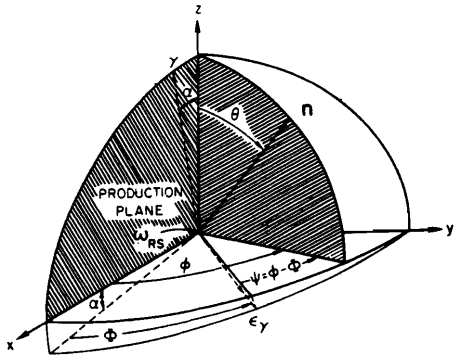

Fig. 9
Definition of polar and azimuthal angles describing the decay of ω into $\pi^+\pi^-\pi^0$ and the observed angular distributions for the events in the ω mass range with polarization of the incident photon >0.3; $\langle P_\gamma \rangle$, the mean polarization, was 0.48.

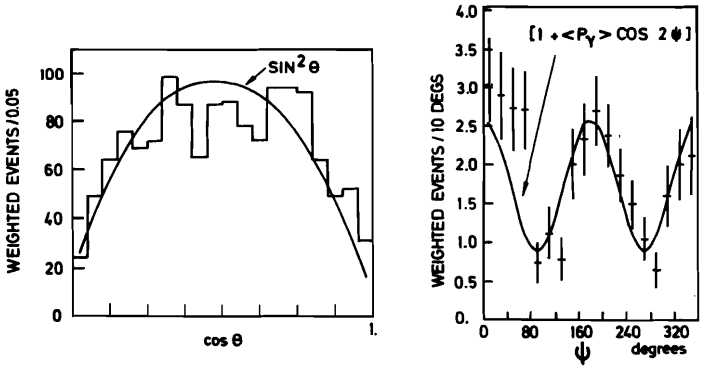

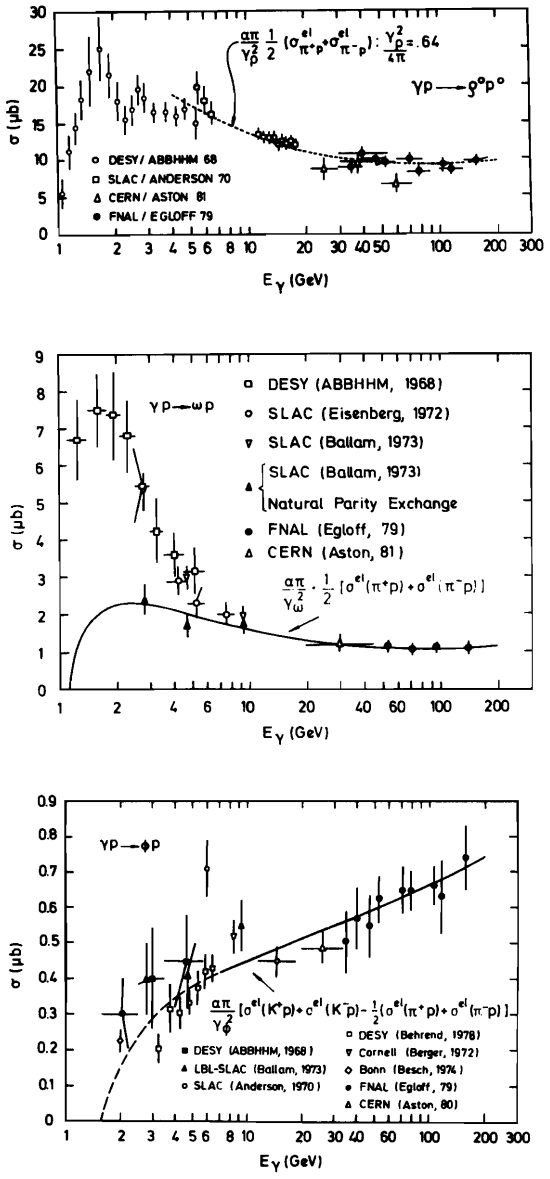

Fig. 10 Total cross sections of elastic ρ^0, ω and ϕ photoproduction as a function of the photon energy (from ref. /21/ with additional results from refs. /8/ and /15/). The curves correspond to quark model predictions deduced from mesonic elastic cross sections /22/ (see text).

scattering at high energies /22/ by assuming naive quark model relations. The curves are normalized to the high energy data /14/. We note that these predictions describe well the energy dependence of the cross sections suggesting that the vector meson-photon coupling strengths do not vary with energy. In fact, these coupling strengths were in turn determined from the normalizations. (They are discussed further in sect. 2.4).

The comparison with hadronic data in the framework of the quark model was extended to the details of the t distributions /8/. Figure 11a shows a compilation of slope parameters b determined in a fit to the t distributions according to $d\sigma/dt \propto \exp(-b|t| + ct^2)$ for recent high energy data on ρ^o and ω photoproduction within similar t ranges. Lower energy ρ^o data are also included. The comparison with the quark model prediction (which is of course identical for ρ^o and ω) shows fair agreement. The parameters c are also consistent with the predictions from corresponding hadronic data.

For the elastic ϕ photoproduction, hadronic data predict a slight shrinkage of the slope parameter b. As fig. 11b shows, the available measurements are still too poor to test this interesting prediction.

2.4 Vector meson-photon coupling strength

We consider first the vector meson-photon coupling in e^+e^- annihilations. In the quark picture the vector meson-photon coupling strength depends on the electric charges of the quarks:

$$\frac{4\pi}{\gamma_V^2} \propto \left(\sum_{q \in V} e_q \right)^2$$

In order to fold out this dependence one has to scale by $(\Sigma e_q)^2$, i.e. by 1/2 for ρ, 1/18 for ω, 1/9 for ϕ etc.

The scaled partial leptonic width related according to (2) by

$$\frac{\Gamma(V \to e^+e^-)}{(\Sigma e_q)^2} = \frac{\alpha^2}{12} \cdot \frac{4\pi/\gamma_V^2}{(\Sigma e_q)^2} \cdot m_V$$

is shown in fig.12. In the case where the scaled coupling strength is mass-independent the scaled $\Gamma(V \to e^+e^-)$ would rise linearly with mass. As one sees the data agree better with an approximately mass independent scaled partial leptonic width. This fact which has been noticed previously /23/, is now also confirmed by the $\Upsilon(9460)$ value.

In fig.13 the vector meson-photon coupling constants obtained from photoproduction data are compared with the corresponding values from e^+e^- annihilations calculated from the partial leptonic widths as shown in fig.12. The values of vector meson-photon coupling constants considered here were obtained from experiments on photoproduction of vector mesons on complex nuclei (independent of quark models, but depending on Glauber theory /19/), and from the normalizations of the predictions to the high energy data in fig. 1o (where a simple quark model was implied).

The ρ^o (not shown) has a set of values from both e^+e^- annihilations and photo-

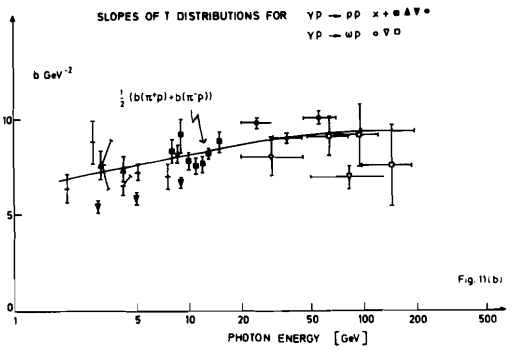

Fig. 11a Slope parameters b of t-distributions of elastic ρ^0 and ω photoproduction as a function of the photon energy (taken from ref. /8/). The curve corresponds to a quark model prediction deduced from πp elastic data /22/.

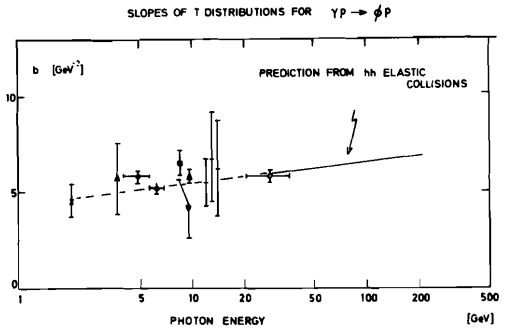

Fig. 11b Slope parameters b of t-distributions of elastic ϕ photoproduction (taken from ref. /15/). The curve corresponds to a quark model prediction deduced in ref. /22/.

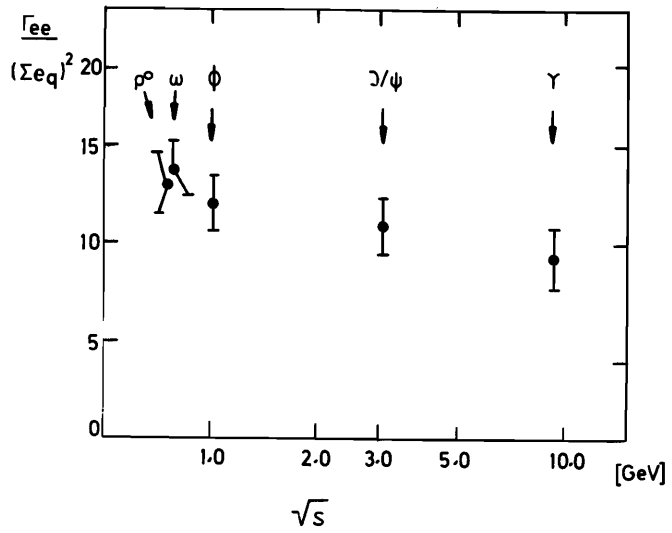

Fig. 12 Partial leptonic widths of vector mesons /34/ scaled according to the electric charges of the quark content.

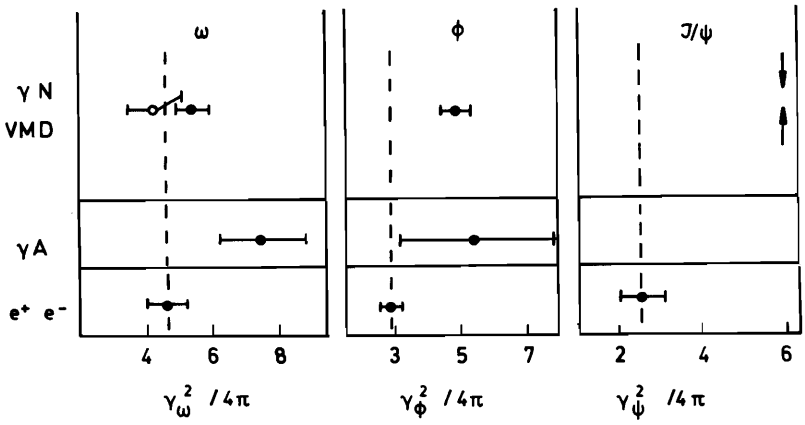

Fig. 13 Comparisons of vector meson-photon coupling constants obtained from e^+e^- annihilations (with the data from fig. 12) and from photoproduction on complex nuclei /24/ and on hydrogen (full points result from fig. 10, the open circle results from the ratio of elastic ω to ρ^0 photoproduction /24/, the arrows mark the estimate explained in the text).

production consistent within the errors of about 15%. The value from ω photoproduction at high energies is fairly consistent with the value from e^+e^- annihilations. The φ data show a significant difference between photoproduction and e^+e^- annihilations which was already noticed in φ photoproduction at lower energies[1] /19, 24, 25/. This difference seems to be even more pronounced in the case of the J/Ψ where a coupling strength estimated from photoproduction data via relation (3), imposing σ(J/ΨN) from a measurement on complex nuclei /26/ is bigger by a factor 2.5 than that from e^+e^- annihilations (fig. 13). These facts suggest that photon-hadron interactions of real photons ($Q^2=0$) are not compatible with those of virtual massive photons in e^+e^- annihilations ($Q^2=m_\gamma^2$).

Various explanations have been discussed in the literature for a long time (see e.g. ref./25/). Newer and rather appealing suggestions analyse this phenomenon in terms of a Q^2 dependence of the vector meson-photon coupling strength /27, 28/. In a contribution to this conference /29/ this coupling is examined in an analysis of the decay $J/\psi \to \eta\gamma$ using VMD along with the quark model and the $\psi' \to J/\psi\ \eta$ width as constraints. The suppression factor for photoproduction found is in the order of five to eight.

2.5 J/ψ photoproduction up to 300 GeV photon energy.

New results on J/ψ photoproduction were submitted to this conference from a Fermilab-Univ. of Illinois experiment using the broad band beam and spectrometer at FNAL /7/. The results of J/ψ production on deuterium and on hydrogen are shown in fig. 14. They indicate a significant rise in the J/ψ cross section over the photon energy range 60 - 300 GeV. The events taken in this experiment represent primarily the sum of elastic J/ψ photoproduction and of processes in which at most the target has fragmented. The fraction of inelastic events was estimated to be about 30%.

Figure 15 shows the differential cross section, dσ/dt, for elastic and inelastic events on hydrogen separately. The curve superimposed on the elastic cross section is a fit to the form $d\sigma/dt \propto \exp(b|t| + ct^2)$ with $b = (-5.7 \pm 0.2)\ GeV^{-2}$ and $c = (3.0 \pm 0.1)\ GeV^{-4}$. A fit to $d\sigma/dt \propto \exp(b|t|)$ yielded a slope of $b = (-3.2 \pm 0.6)\ GeV^{-2}$. The inelastic cross section (with forward going J/Ψ) turns out to have a weaker t dependence, however, error bars are still large.

The forward cross section dσ/dt at t=0 is rising also (fig. 16). The rise, interpreted in the view point of VMD, implies an increase in $\sigma_{TOT}^{J/\psi\ N}$ of 40% from 60 to 300 GeV. Here it was assumed that elastic and inelastic data have the same energy dependence.

3. NEW RESULTS ON ρ'(1600)

3.1 ρ'(1600) in $\gamma p \to 2\pi^+ 2\pi^- p$

The ρ'(1600) is so far the best established candidate of a radial excitation state of the ρ^0. The discovery in the early seventies was based on the production of a system of four charged pions in the two reactions:

Fig. 14
Cross section vs. energy for γ + (p or d) → J/Ψ + X obtained by averaging $\sigma \cdot B(J/\Psi \to \mu^+\mu^-)$ and $\sigma \cdot B(J/\Psi \to e^+e^-)$.

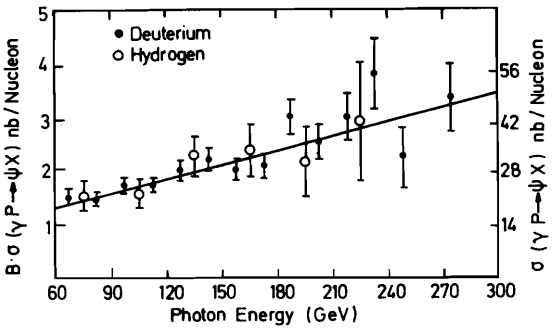

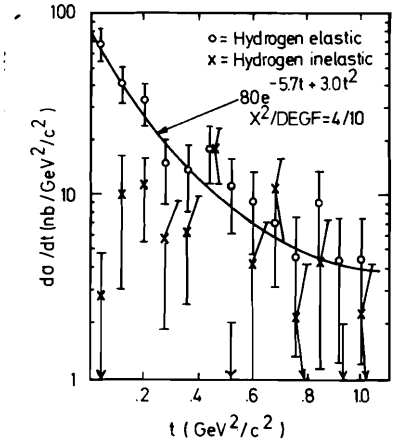

Fig. 15
Differential cross sections, dσ/dt, for J/Ψ photoproduction on hydrogen separated into elastic and inelastic components averaged over energies from 60 to 300 GeV.

Fig. 16
Cross section dσ/dt at t = 0 vs. energy /7/.

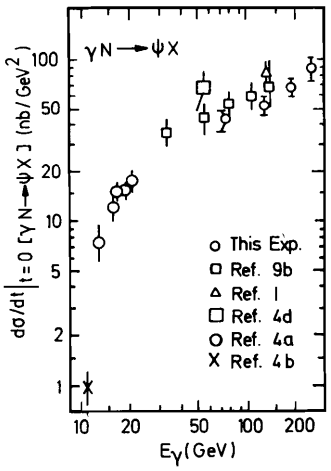

and
$$\gamma p \rightarrow 2\pi^+2\pi^- p$$
$$e^+e^- \rightarrow 2\pi^+2\pi^-$$

The $2\pi^+2\pi^-$ mass spectra from the most recent experiments /31, 6/ are shown in figs. 17a and b. The curve in the photoproduction mass spectrum (Fig. 17a) corresponds to the fit curve in fig. 17b modified by a factor $\{M(2\pi^+2\pi^-)\}^2$ and normalized to the data in the peak region. Mass spectrum and curve are expected to agree in the approximation of simple VMD. The comparison suggests fair agreement in position and width.

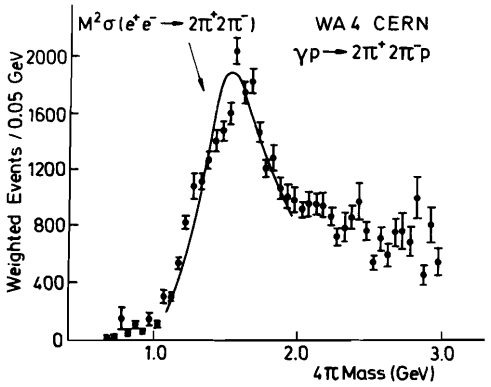

Fig. 17 a

$2\pi^+2\pi^-$ mass spectrum measured in the reaction $\gamma p \rightarrow 2\pi^+2\pi^- p$ /31/. The curve is described in the text.

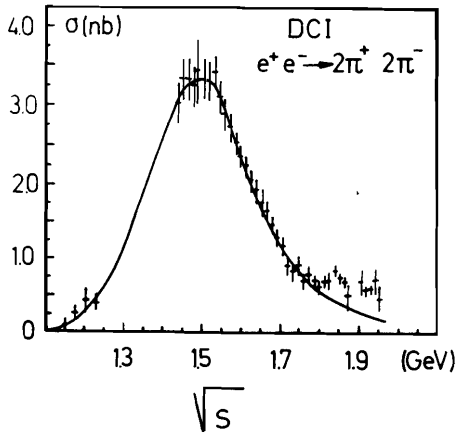

Fig. 17 b

$2\pi^+2\pi^-$ mass spectrum measured in the reaction $e^+e^- \rightarrow 2\pi^+2\pi^-$. The curve is the result from a fit to the data (see ref. /6/).

The other relevant process where a clear bump structure around 1.6 GeV was reported is the photoproduction of $\pi^+\pi^-$. A recent result of $\pi^+\pi^-$ photoproduction on carbon from the broad band photon beam at Fermilab /32/ is shown in fig. 18. This result agrees with another recent measurement of $\pi^+\pi^-$ pair production on hydrogen /33/ and is consistent with certain solutions in $\pi\pi$ phase shift analyses /34/. However, a quantitative comparison between the 4π and the 2π signals in figs. 17 and 18 indicates a serious problem: the apparent widths are inconsistent. Various other experiments with tentative candidates for the $\rho'(1600)$ have parametrized the peak structure. Figure 19 shows a compilation of mean values and widths published during the last four years. One sees a considerable spread of values in mass

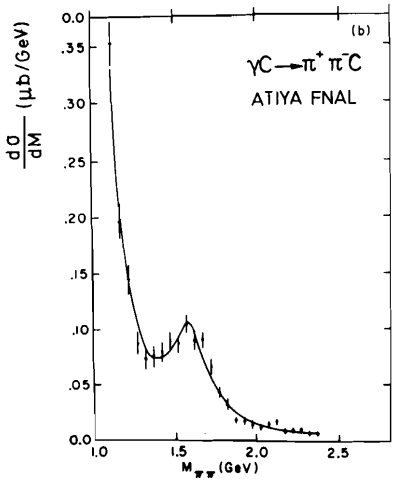

Fig. 18 Mass distribution of the $\pi^+\pi^-$ system observed in the reaction $\gamma C \to \pi^+\pi^- C$ having $p_T^2 \to 0.05$ GeV² (32).

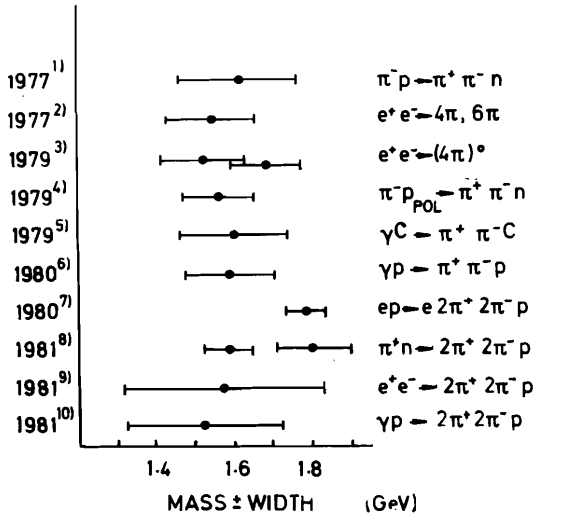

Fig. 19 Masses and widths of structures reported in the four- and two-pion systems. The lengths of the bars indicate the Breit-Wigner widths. 1) ref./35/; 2) ref./36/; 3) ref./37/; 4) ref./39/; 5) ref./32/; 6) ref./33/; 7) ref./40/; 8) ref./41/; 9) ref./6/ and 10) ref./31/.

and width. Two experiments even claim two-peak structures (both with rather low statistics). It has to be noticed that this scattering of results is only partially explained by the differences in the parametrization of the mass-dependent width.

If in photoproduction data the $2\pi^+2\pi^-$ and $\pi^+\pi^-$ signals originate from the same resonance, at least one of them must be deformed by background or interference effects. The $\pi^+\pi^-$ peak sits on the ρ^0 tail which is not well understood via photoproduction and, at the available level of statistics, a more detailed analysis is not possible.

For the $2\pi^+2\pi^-$ peak, which has now been measured with high statistics (fig. 17 a), it is important to separate the resonance signal from threshold effects and other backgrounds. Those are predicted in various models (see for instance /42/). A first step in this direction was tried in an analysis on the data in fig. 17a where the $2\pi^+2\pi^-$ peak was fitted (in kinematical variables) to linear combinations of intensities of various models /31/. Since there is about one ρ^0 in the $2\pi^+2\pi^-$ system of each event (fig. 20), it was assumed that $\rho'(1600)$ produces always a ρ^0 by its decay, and consequently the following models were considered:

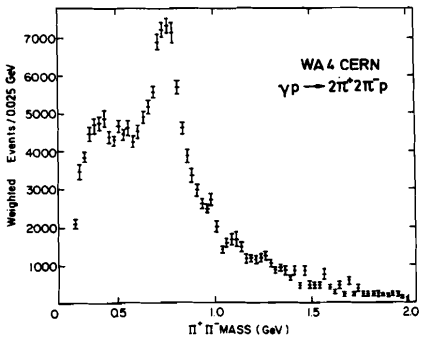

Fig. 20
Mass distribution of the $\pi^+\pi^-$ system observed in the reaction $\gamma p \to 2\pi^+2\pi^- p$ for $M(2\pi^+2\pi^-) < 3.05$ GeV.

model 1 $\quad \rho'(1600) \to$ "$A_1^{\pm}$" $\pi^{\mp}$, "A_1" $\to \rho^0\pi^{\pm}$, $\rho^0 \to \pi^+\pi^-$

where "A_1" stands for a $\rho\pi$ system in s-wave with a wide $\rho\pi$ mass spectrum around 1.3 GeV.

model 2 $\quad \rho'(1600) \to \rho^0\varepsilon$, $\rho^0 \to \pi^+\pi^-$, $\varepsilon \to \pi^+\pi^-$

where ε was described by measured s-wave $\pi\pi$ phase shifts /34/.

The details of this analysis are given in ref. /31/.
As already reported at previous conferences /43, 44/, successful fits were obtained with either of the two models. In particular, it was found that about 60 % of the $2\pi^+2\pi^-$ peak in fig. 17a could be due to the resonance while the remainder is described by background contributions like $\rho\pi\pi$ phase space or 4π phase space.
This analysis does not tell us what the relative importance of the two possible decay modes $\rho'(1600) \to$ "A_1"π and $\rho'(1600) \to \rho^0\varepsilon$ might be, since there is no unique signature in the $\rho^0\pi^+\pi^-$ final state for distinguishing them.

3.2 $\rho'(1600)$ in $\gamma p \to \pi^+\pi^-\pi^0\pi^0 p$

More insight into the $\rho'(1600)$ comes from a new measurement of the $\pi^+\pi^-\pi^0\pi^0$ system in photoproduction, where both neutral pions were measured with high efficiency /9/. In these data the two decay models of the $\rho'(1600)$ considered already for the charged four-pion system are clearly distinguished from each other by the ρ production:

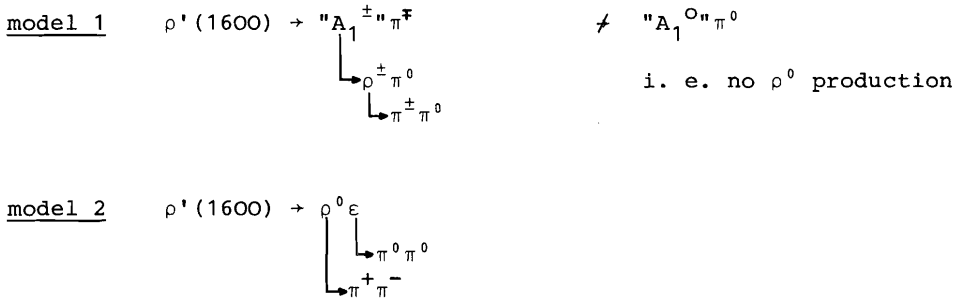

The $\pi^+\pi^-\pi^0\pi^0$ mass spectrum (fig. 21) shows two peaks:

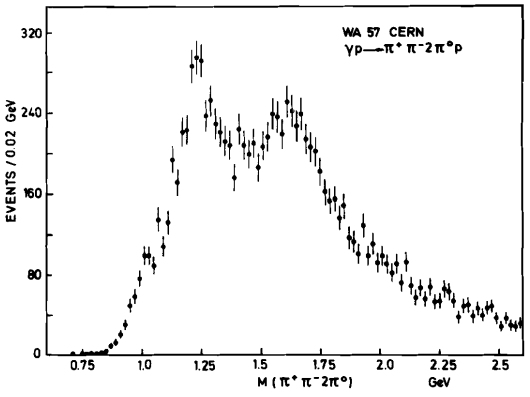

Fig. 21
Effective mass spectrum for $\pi^+\pi^-\pi^0\pi^0$ observed in the reaction $\gamma p \to \pi^+\pi^-\pi^0\pi^0 p$ /9/

The lower peak particularly corresponds to the production of the $\omega\pi^0$ state and was analysed separately /12/, (see section 4). The higher mass peak suggests the presence of the $\rho'(1600)$ with a decay into $\pi^+\pi^-\pi^0\pi^0$. (This two-peak structure was already seen in a previous measurement of $\gamma p \to p\pi^+\pi^-$ + neutrals where the neutrals (π^0's) were not reconstructed /45/.)

Two-pion mass spectra of the events in the $\rho'(1600)$ mass range (fig. 22) show clearly that there is dominant production of $\rho^\pm$ and only little ρ^0. This was studied quantitatively by fitting the data in slices of the $\pi^+\pi^-2\pi^0$ mass spectrum to a sum of simulated contributions (neglecting interferences) including the two models for the $\rho'(1600)$ decay plus $\omega\pi^0$ and various phase space-like

backgrounds.

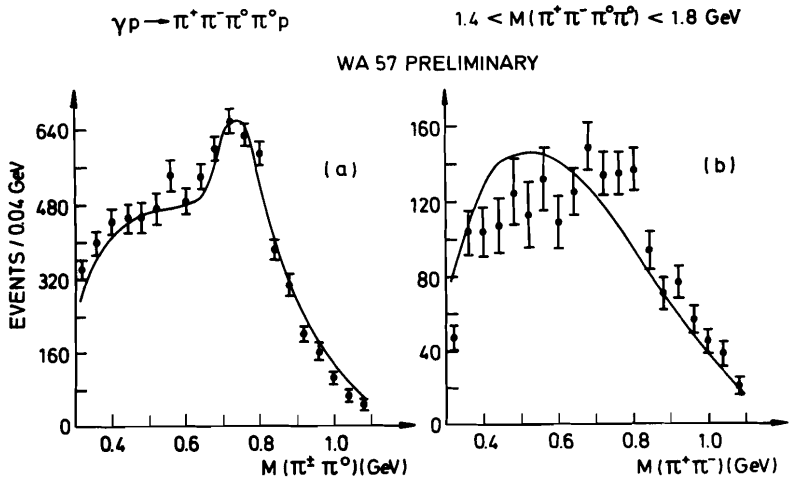

Fig. 22
Measured two-pion mass spectra from $\gamma p \to \pi^+\pi^-\pi^0\pi^0 p$ for $1.4 < M(\pi^+\pi^-\pi^0\pi^0) > 1.8$ GeV. with $\omega\pi^0$ contribution subtracted, for (a) $\pi^\pm\pi^0$, (b) $\pi^+\pi^-$. The curves result from a fit to the $\pi^\pm\pi^0$ mass spectrum /44/.

As a result, fig. 23 shows the intensities of the three major contributions which, in this case, represent together the $\pi^+\pi^-\pi^0\pi^0$ mass spectrum.

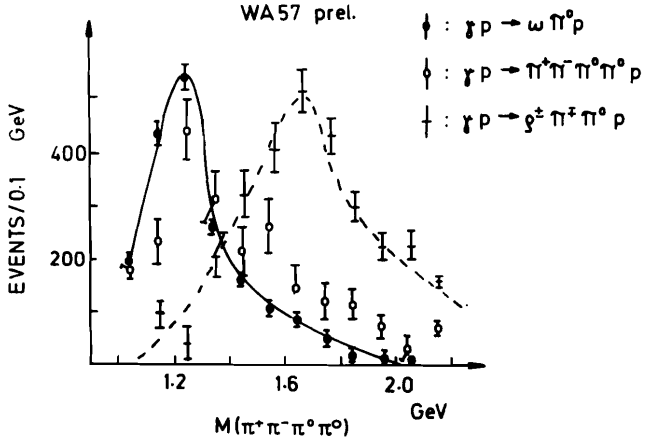

Fig. 23
Fitted yields of $\omega\pi^0$, $\rho^\pm\pi^+\pi^0$ and $\pi^+\pi^-\pi^0\pi^0$ phase space. The curves are hand-drawn.

The upper mass peak corresponds to the production of the $\rho^\pm\pi^\mp\pi^0$ state. This clearly favours model 1. There is no need for model 2. The $\rho\varepsilon$ component was estimated to be of a relatively small size:

$$\frac{\rho'(1600) \to \rho^0\pi^0\pi^0}{\rho'(1600) \to \rho^\pm\pi^\pm\pi^0} < 0.15$$

This result which is not very sensitive to the details of the fitting procedure, rules out $\rho\varepsilon$ as dominant decay mode of the $\rho'(1600)$.

3.3 $\rho'(1600)$ in $\gamma p \to \eta\pi^+\pi^- p$

In another paper submitted to this conference /10/ the OMEGA-Photon Collaboration has studied the possible $\eta\pi^+\pi^-$ decay mode of the $\rho'(1600)$. In this experiment (WA 57) the η was observed nicely in its decay into $\gamma\gamma$ (fig. 24) as well as in the $\pi^+\pi^-\pi^0$ decay mode. The $\eta\pi^+\pi^-$ mass spectrum (from data added for both η decay modes) shows again a two-peak structure (fig. 25).

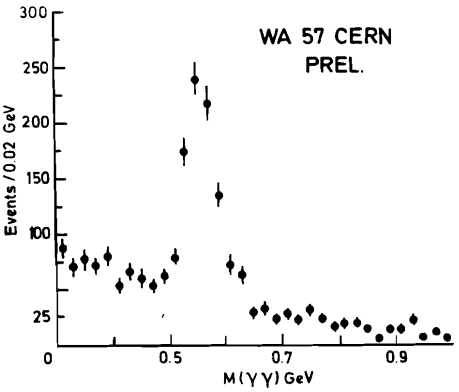

Fig. 24
The $\gamma\gamma$ mass spectrum with the η meson signal in the reaction $\gamma p \to \eta\pi^+\pi^- p$ /10/

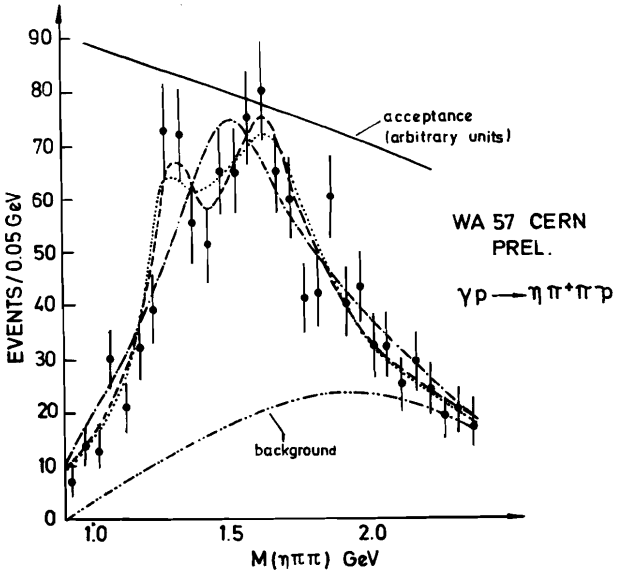

Fig. 25
The $\eta\pi^+\pi^-$ mass spectrum for the reaction $\gamma p \to \eta\pi^+\pi^- p$ selecting for events in the η meson peak. -·-·- example of a fit with one resonance plus background; ---- example of a fit with two resonances plus background giving $M_1 = 1.301 \pm 0.031$ GeV, $\Gamma_1 = 0.2$ GeV (fixed), $M_2 = 1.623 \pm 0.016$ GeV, $\Gamma_2 = 0.4$ GeV (fixed) with $\chi^2 = 29.8$ for 22 d.o.f; ·-·- polynomial background of this fit; ···· example of a fit with two resonances (lower distorted by $\eta\rho^0$ threshold) plus background.

The fit to the $\eta\pi^+\pi^-$ mass spectrum with only one resonance gives a poor χ^2 probability. Fits with a sum of two non-interfering resonances (plus a cubic polynomial background) describe the mass spectrum well. These fits were of two classes: without and with distortion of the lower peak by the $\eta\rho^0$ threshold.The higher mass peak was consistent with the $\rho'(1600)$ as observed in 4π decay modes. The branching ratio is

$$\frac{\rho'(1600) \to \eta\pi^+\pi^-}{\rho'(1600) \to \pi^+\pi^-\pi^+\pi^-} \sim 0.1$$

which agrees with a rough estimate on e^+e^- annihilation data/6/. The lower mass peak is centred at about 1.3 GeV. With distortion by the $\eta\rho^0$ threshold it was found that the "true" mass value could be at 1.23 GeV raising the possibility of it being a decay mode of the B(1235) meson. A study on the angular distributions should shed more light on this point.

3.4 Photon coupling of $\rho'(1600)$ in e^+e^- annihilations

Within the context of the $\rho'(1600)$ being a candidate of a radial excitation state of the ρ^0 it is desirable to understand the strength of the coupling to the photon. An estimate of the related partial leptonic width was obtained at DCI/6/ by adding ($\Gamma(\rho'(1600) \to e^+e^-)$ · branching ratio) for $2\pi^+2\pi^-$ and some other minor decay modes and correcting for unobserved $\rho'(1600)$ decay modes by means of SU(3) relations. The resulting value of about 7 keV is compared to the ρ^0 and to corresponding states in the J/ψ and T families in fig. 26 where the partial leptonic

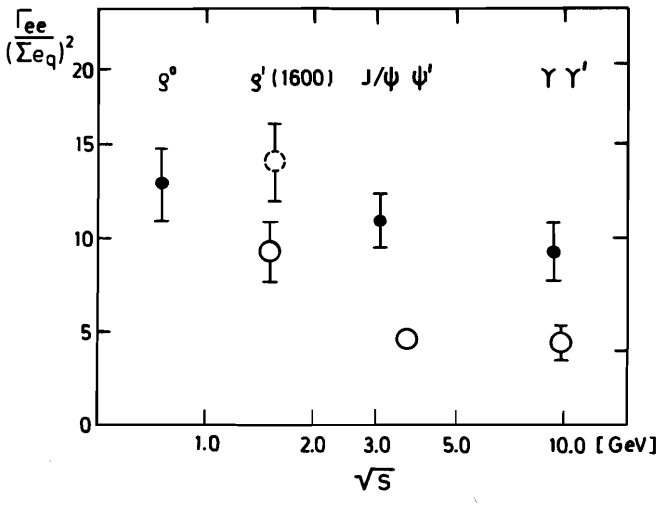

Fig. 26 Partial leptonic widths of vector mesons and the candidates of first radial excitation states scaled according to the electric charges of the quark content. For the $\rho'(1600)$ values see text. $\psi' \equiv \psi(3685)$; $T' \equiv T(10020)$; full points: ground states, open circles: 1. radial excitations.

widths, again scaled according to the quark contents of the states, are drawn. The DCI result (dashed line symbol) is rather high. If one applies plausible corrections, mainly for a substantial non-resonant background under the $\rho'(1600)$ signal in $e^+e^- \to 2\pi^+2\pi^-$ as found in photoproduction and by neglecting $\rho'(1600) \to \omega\pi^0$ (as it is suggested due to fig. 23) one obtains a "best guess" which is

significantly lower(full line symbol). However, it is not as low as

$$\frac{\Gamma(\rho^0 \to e^+e^-)}{(\Sigma e_q)^2} \cdot \frac{\Gamma(\Upsilon(10020) \to e^+e^-)}{\Gamma(\Upsilon(9460) \to e^+e^-)}$$

which one would expect in the case where the ratio of coupling strengths between ρ' and ρ is equal to that between ψ' and J/ψ or Υ' and Υ.

3.5 Summary of results on $\rho'(1600)$

The $\rho'(1600)$ was studied in recent experiments in the four-pion decay channels $2\pi^+2\pi^-$ and $\pi^+\pi^-2\pi^0$ and was probably seen in the $\eta\pi^+\pi^-$ channel. The width is always large ($\geq$0.4 GeV) in these channels. Due to the principle uncertainties in describing such a wide resonance shape it is an unsolved problem to extract important parameters like mass, width and, from cross sections, the partial leptonic width.

The $\rho'(1600)$ decays dominantly into $\rho\pi\pi$ through an"A_1"π state where"A_1" indicates an $I^G = 1^-$ state. $\rho\varepsilon$ is eliminated as the dominant decay mode of the $\rho'(1600)$.

4. THE $\rho'(1250)$ PUZZLE

A $\rho'(1250)$ state is predicted by various models. For instance, it is required by the isovector part of the nucleon form factor/46/.

4.1 Bump structures

An experimental result which stimulated the discussion about existence or non-existence of the $\rho'(1250)$ is the pion form factor shown in fig. 27 which exhibits a bump above the ρ^0 tail at a mass of about 1.25 GeV.

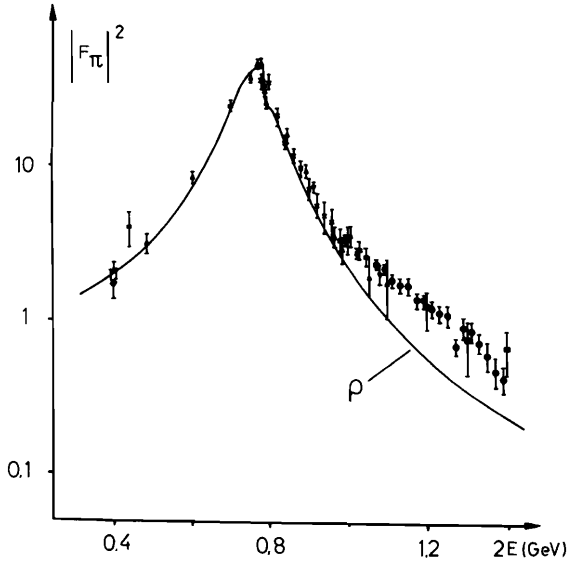

Fig. 27 Compilation of measurements of the pion form factor taken from ref./47/.

More recently the charged kaon form factor was measured /13/. The data (fig. 28) is compatible with a broad bump structure above the $(\rho^0+\omega+\phi)$ tail ranging from about 1.2 to 1.7 GeV. Comparisons with models are not very conclusive at the moment /48/.

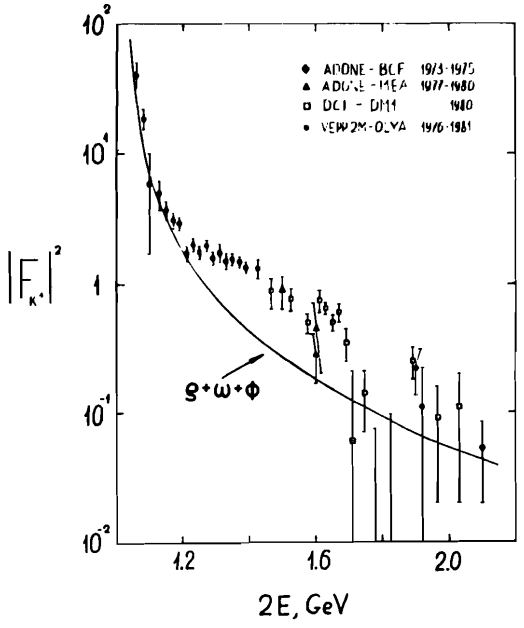

Fig. 28 Compilation of measurements of the charged kaon form factor/13/.

More data are required; in particular, measurements of the neutral kaon form factor are needed in order to decompose the $K\bar{K}$ isospin configuration.

4.2 Missing evidence

As negative results the present $\pi\pi$ phase shifts and the results from photoproduction of two and four charged pions do not require the existence of a substantial $\rho'(1250)$ state.

Figure 29 shows a compilation of cross sections of the reaction $e^+e^- \to \pi^+\pi^-2\pi^0$ presented by Sidorov at the last Photon-Lepton-Conference /47/. The data come from four experiments at the e^+e^- storage rings in Orsay, Frascati and Novosibirsk. The full line corresponds to the measurement of $e^+e^- \to 2\pi^+2\pi^-$ /6/. Assuming that $\rho'(1600)$ decays dominantly through an $A_1\pi$ type state as suggested by the data (see sec. 3) then $\sigma(e^+e^- \to \pi^+\pi^-\pi^0\pi^0)$ and $\sigma(e^+e^- \to \pi^+\pi^-\pi^+\pi^-)$ are expected to agree in shape and normalization, provided that other contributions are unimportant or equal in both channels[2]. Previous discussions /49/ assumed a dominant $\rho\varepsilon$ decay mode for the $\rho'(1600)$ and therefore compared $\sigma(e^+e^- \to \pi^+\pi^-2\pi^0)$ with 1/2 $(e^+e^- \to 2\pi^+2\pi^-)$. In fig. 29 it is seen that data and dashed curve agree in the peak region of the $\rho'(1600)$ and at higher masses; however there is a possible excess in favour of

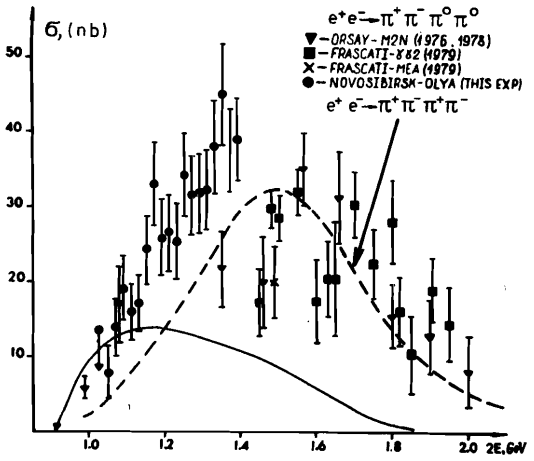

Fig. 29 Compilation of measured cross sections on the reaction $e^+e^- \to \pi^+\pi^-\pi^0\pi^0$ as function of the energy (taken from ref./47/). Solid curve represents the $\omega\pi^0$ contribution from ρ^0 decay, taken from ref./50/.

$e^+e^- \to \pi^+\pi^-2\pi^0$ at the lower masses. If this excess is real and not due to a systematic effect in the normalization (all the corresponding data belong to one experiment /47/) one must find out next whether it is consistent with the tail of the ρ^0 predicted to contribute to $\pi^+\pi^-2\pi^0$ through the $\omega\pi^0$ state /50/ and probably also through an $A_1\pi$ type state[3]. My impression is that there is no obvious need for $\rho'(1250)$ at present.

4.3 Spin parity analysis of the $\omega\pi^0$ system in $\gamma p \to \pi^+\pi^-\pi^0\pi^0 p$

A new piece of the $\rho'(1250)$ puzzle comes from the OMEGA-Photon Collaboration who have looked for the $\rho'(1250)$ in the photoproduced $\pi^+\pi^-\pi^0\pi^0$ system /12/. The $\pi^+\pi^-\pi^0\pi^0$ mass spectrum (fig. 21) contains a peak at $\sim$ 1.25 GeV which is mainly built up by $\omega\pi^0$ states since a selection on events with a $\pi^+\pi^-\pi^0$ combination in the ω mass range (fig. 30) reproduces this peak (fig. 31).

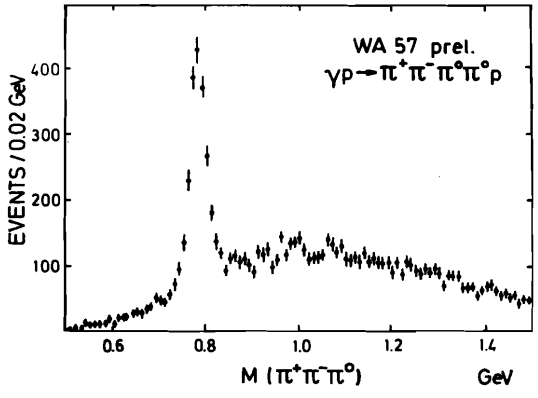

Fig. 30 The $\pi^+\pi^-\pi^0$ effective mass spectrum observed in the reaction $\gamma p \to \pi^+\pi^-\pi^0\pi^0 p$ /12/.

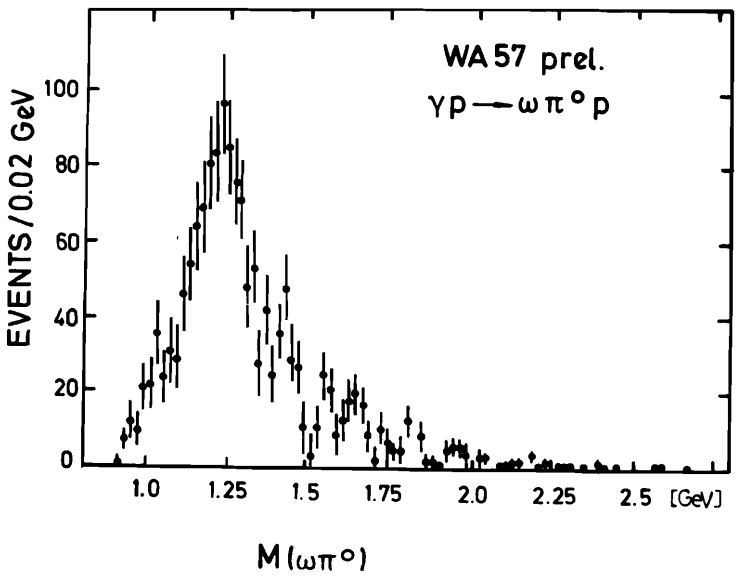

Fig. 31 $\omega\pi^0$ mass spectrum observed in the reaction $\gamma p \to \omega\pi^0 p$.

The events thus selected were analyzed to determine the spin-parity of the $\omega\pi^0$ system. The decay of this system is described by four angles, two belonging to the ω in the $\omega\pi^0$ rest system and two to the normal on the ω decay plane in the ω rest system as indicated in fig. 32. Figure 33 shows the experimental distributions of these angles. They were analyzed in terms of certain moments /52/ forming a complete set for the description of the distributions arising from $\omega\pi^0$ spin-parities 0^-, 1^- and 1^+.

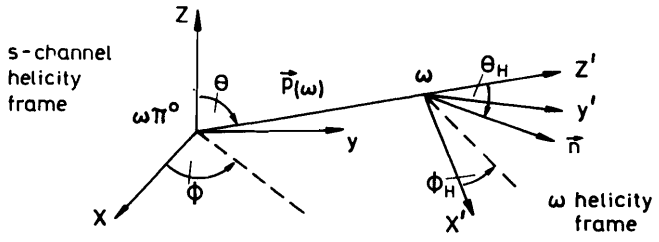

Fig. 32 Definition of the angles used to describe the production and decay of the $\omega\pi^0$ system.

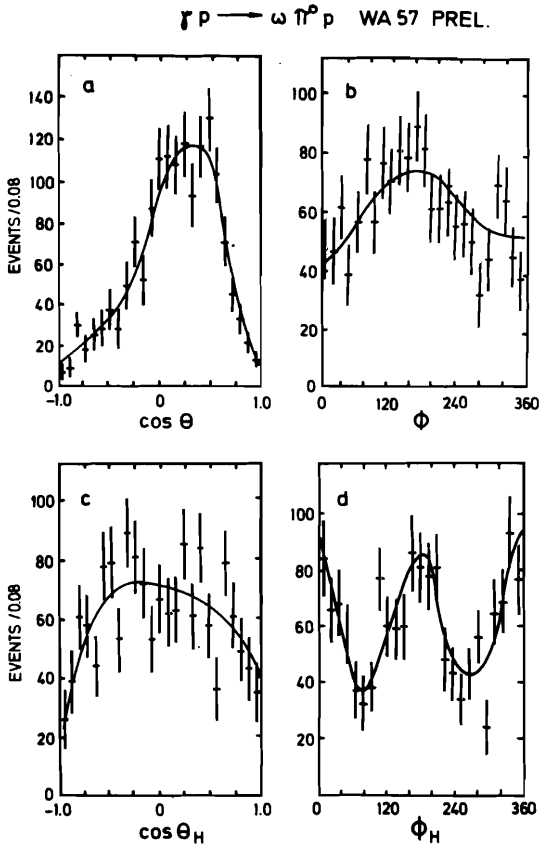

Fig.33
Measured distributions of a) cos θ, b) ϕ, c) cos θ_H and d) ϕ_H from reaction $\gamma p \to \omega\pi^0 p$. The curves shown are obtained from the moments folded with acceptance (see text).

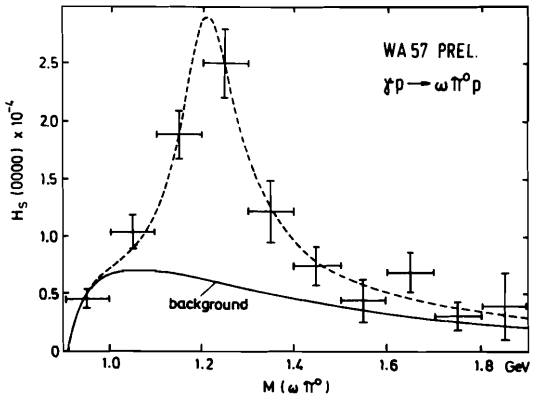

Fig. 34
The $\omega\pi^0$ mass spectrum (corrected for acceptance). The dashed curve corresponds to a fit (see text).

The angular distribution predicted in turn from these moments served as a check that it is sufficient to consider only 0^-, 1^- and 1^+ as the spin parities of the $\omega\pi^0$ system (curves in figs. 33 a and b). The curves in figs. 33 c and d show that the data reproduce the imposed spin parity of the ω system ($J^P = 1^-$).

The lowest moment corresponding to the $\omega\pi^0$ mass spectrum (corrected for acceptance losses) was fitted to a relativistic Breit-Wigner with mass-dependent width and a background term (fig. 34) yielding the resonance parameters:

$$m_R = 1.212 \pm 0.012 \text{ GeV} \qquad \Gamma_R = 0.154 \pm 0.07 \text{ GeV}$$

These parameters are in agreement with those of the B(1235) meson which has $J^{PC} = 1^{+-}$ and could indeed be produced diffractively in photoproduction by analogy with diffractive A_1 production in πp collisions.
As a first step towards a full analysis the possible spin-parities of the $\omega\pi^0$ system were restricted to 1^- and 1^+ since 0^- was found to be a small contribution. Two types of fits were tried:

FIT 1 assuming s-channel helicity conservation (SCHC) in the production mechanism of the 1^- component

and

FIT 2 without this assumption.

The preliminary results (based on the moments which do not depend upon interference between 1^- and 1^+) are summarized in fig. 35.

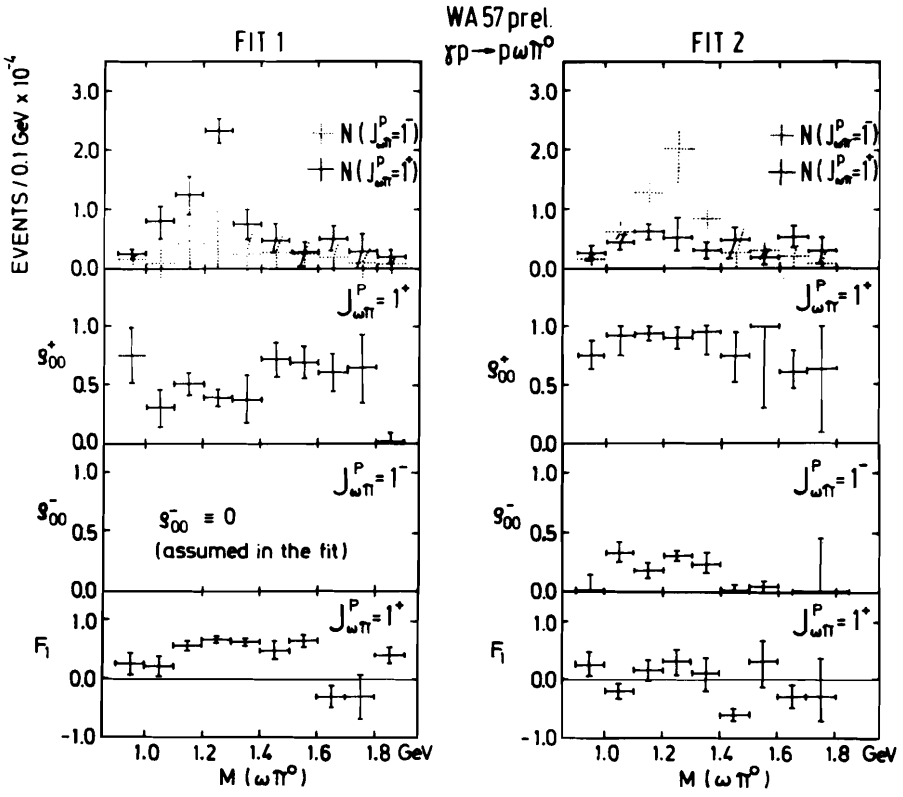

Fig. 35
Parameters of the $\omega\pi^0$ spin-parity states 1^+ and 1^- as a function of the $\omega\pi^0$ mass as obtained in two distinct fits to the data (see text).

The first row containing the intensities of 1^- and 1^+ as a function of the $\omega\pi^0$ mass shows that in FIT 1 (with SCHC constraint for 1^-) the 1^+ component clearly dominates over 1^- in the peak region (at ~ 1.25 GeV) while in FIT 2 (without this constraint) the peak is dominated by the 1^- component.

The other rows give further details of the fit results: the spin density matrix elements ρ_{00} of the 1^- and 1^+ components which must vanish in the case of SCHC, F_1 is the helicity 1 amplitude of the ω for the 1^+ component which is a measure of the ratio of s-wave to d-wave in the $\omega\pi^0$ system.
In FIT 1 the dominant 1^+ component is in agreement with the B(1235), in particular F_1 is fully consistent with the table value 0.67 ± 0.01 for the B(1235) /34/. Assuming that this fit provides the correct interpretation of the data, the non-vanishing ρ_{00} shows that for the production of 1^+ s-channel helicity is not conserved. In the alternative case that FIT 2 is true, the dominant 1^- component has $\rho_{00} \neq 0$ within the peak region which means that there is no agreement with the common expectation of SCHC in diffractive photoproduction of vector mesons. This is a somewhat peculiar fact which needs further investigation. There is certainly no final conclusion at this preliminary stage of the spin-parity analysis. In the near future there will be more detailed results since there are more data in the WA 57-experiment (by a factor of two). The final analysis will include the full experimental information contained in the moments describing the interference between the states of different spin or parity and perhaps also the partial polarization of the incident photons.

4.4 Summary of results for $\rho'(1250)$

There are at present no data which require the existence of the $\rho'(1250)$. The search for $\rho'(1250)$ in photoproduction of $\omega\pi^0$ yields as a preliminary result two solutions:

either	the $\omega\pi^0$ peak is dominantly due to B(1235) and there is no need for a resonant $J^P = 1^-$ state.
or	the $\omega\pi^0$ peak corresponds to a strong $J^P = 1^-$ signal which may be a candidate for the $\rho'(1250)$, however, at the moment with a question mark because of non-SCHC.

5. SEARCH FOR ϕ' AND ω'

5.1 The $\phi'(1650)$ candidate

Among the various isoscalar candidates which have been discussed at previous conferences, one has now reached a somewhat increased level of confidence due to extensive measurements with the DM1 spectrometer at DCI. This candidate is called $\phi'(1650)$ and Dr. Delcourt has presented the current status in the preceding talk.
It was found in the analysis of the DCI data that $e^+e^- \to \bar{K}K\pi$ going mainly through $K^*\bar{K}$ ($\bar{K}^*K$) is the dominant decay mode of the $\phi'(1650)$ /6/. The argument is based on the isospin decomposition of the K^*K system, which was obtained with relatively small statistics (fig. 36).

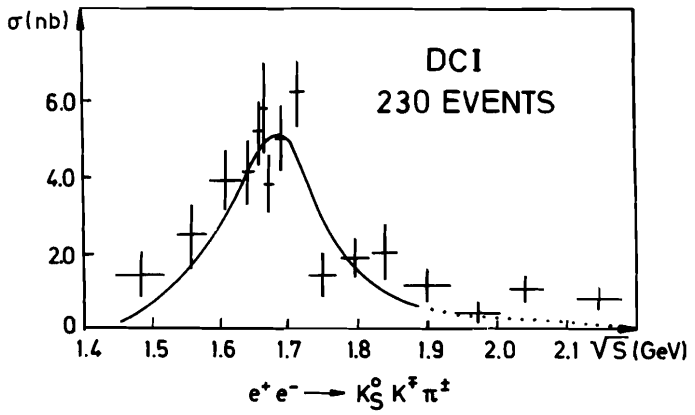

Fig. 36 The measured cross section σ ($e^+e^- \to K_S^0 K^{\pm}\pi^{\mp}$) as a function of the energy /6/.

It certainly needs confirmation but at present there are no higher statistics data available. Figure 37 shows a first result from photoproduction of $K\bar{K}\pi$. The curve corresponds to the curve in fig. 36 modified by a factor $|M(K\bar{K}\pi)|^2$ with arbitrary normalization. There is no obvious peak structure at a mass of 1.65 GeV.

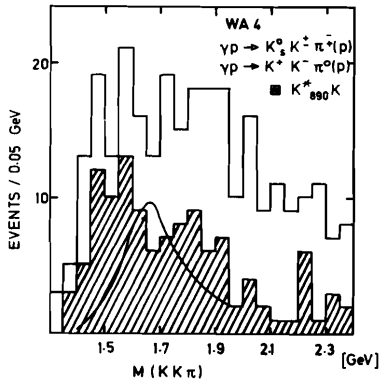

Fig. 37 The $K\bar{K}\pi$ mass spectrum measured in the reactions $\gamma p \to K_S^0 K^+\pi^{\pm}$ or $\gamma p \to K^+K^-\pi^0$. The curve is explained in the text.

Conclusions cannot be drawn without more details(spin-parity and isospin of the $K\bar{K}\pi$ system) which are hardly accessible in photoproduction at this low statistical level.

Some support for a $\phi'(1650)$ was reported from photoproduction of K^+K^- pairs /54/ where a signal was observed in the K^+K^- mass spectrum centred at a slightly higher mass value (fig. 38). This peak is consistent with the $\phi'(1650)$ provided that the shift in the mass can be explained by interference effects. However, the interference structure could not be analyzed completely (there is a principle complication due to an arbitrariness in the relative phases) so that there is no

proof of this interpretation at present.

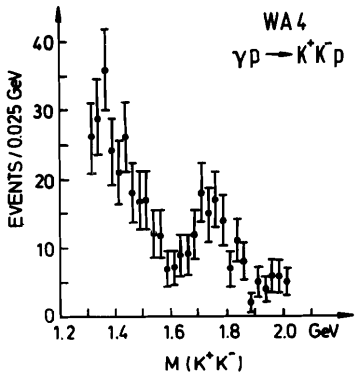

Fig. 38 The K^+K^- mass spectrum observed in the reaction $\gamma p \to K^+K^-p$ /54/.

5.2 A bump at 1.68 GeV in the $\pi^+\pi^-\pi^0$ system

A signal at a mass of 1.68 GeV is observed in a measurement of $\pi^+\pi^-\pi^0$ photoproduction /11/. (This experiment was discussed already with respect to ω in sec. 2 Figure 39a shows the $\pi^+\pi^-\pi^0$ mass distribution in the range from 1.2 to 2.2 GeV with evidence for a peak at 1.68 GeV. This peak has also been observed in a preceding photoproduction experiment /44/ (fig. 39b). Moreover, weaker peaks at this

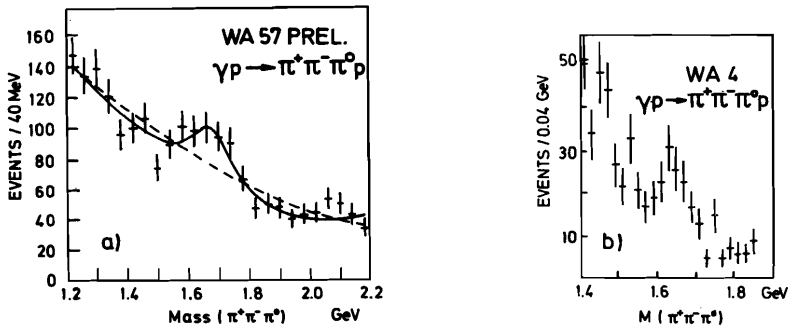

Fig. 39 The $\pi^+\pi^-\pi^0$ mass spectrum around a mass of 1.7 GeV observed in the reaction $\gamma p \to \pi^+\pi^-\pi^0 p$, in a) from experiment WA 57 /11/ and in b) from experiment WA 4 /44/. The curve in a) is explained in the text.

mass are reported from previous measurements of $e^+e^- \to \pi^+\pi^-\pi^0$ at DCI /38/ and ADONE /55/. A simple fit to the mass spectrum in fig. 39a yields

$m_R = 1.68 \pm 0.02$ GeV $\Gamma_R = 0.15 \pm 0.02$ GeV and $\sigma_R = (140 \pm 40)$ nb.

The statistical significance of the peak counted above the background curve is 4.3 σ.

An identification of this signal remains speculative. It is probably too narrow for a radial excitation of the ω. It could indicate a $\pi^+\pi^-\pi^0$ decay of the $\phi'(1650)$. However, assuming this case, the large photoproduction cross section would suggest a serious violation of the OZI rule. An estimate of the branching ratio obtained from this data (via relation (3)) by assuming

$\Gamma(\phi'(1650) \to e^+e^-) = 0.8$ keV /6/ and $\sigma(\phi' p) = 10$mb points to a value which is much larger than the current estimate of $< 10\%$ for $\phi'(1650) \to 2\pi^+2\pi^-\pi^0$ obtained from e^+e^- annihilation /6/. As far as photoproduction is concerned there is another possible interpretation: the peak could be due to the $\omega'(1650)$ with $J^{PC} = 3^{--}$.

6. SUMMARY AND CONCLUSIONS

In summary I would like to make the following remarks:

1) Elastic photoproduction of ρ^0, ω and ϕ at high energies is described well by simple Vector Meson Dominance making use of naive quark model relations and the experimental data on elastic scattering of pions and kaons at high energies. A possible Q^2 dependence of the vector meson-photon coupling strengths is discussed.
2) New data on J/Ψ photoproduction indicate a significant rise in the cross section over the photon energy range 60 to 300 GeV.
3) Among the candidates for radial excitations of the ρ^0 the $\rho'(1650)$ is established. If it is the <u>first</u> excited state, then its mass difference to the ground state of about 0.86 GeV is certainly larger than found in the heavy quark families. However, the existence of the $\rho'(1250)$ is not ruled out at present.
4) In the search for isoscalar radial excitations the $\phi'(1650)$ candidate was found in e^+e^- annihilations, but needs confirmation.

ACKNOWLEDGMENTS

I am very grateful to my Bonn colleagues, especially to B. Diekmann, K. Heinloth, W. Pfeil, and H. Raszillier for many discussions and for help during the preparation of this report. Also I would like to thank warmly all my colleagues in the OMEGA-Photon Collaboration for their cooperation and support.

References

/1/ See for instance:
R.Taylor, Proc. 1975 Int.Symp. on Lepton and Photon Interactions at High Energies (SLAC-Pub., Stanford 1975) p. 679;
S.B.Gerasimov, Effective Interactions of Quarks and Static Properties of Hadrons, Dubna E2-81-268;
A.Martin, Int. Conf. on High Energy Physics of the European Physical Society, Lisbon 1981, in preparation.

/2/ For a recent summary see:
L.Montanet, Proc. XX. Int. Conf. on High Energy Physics, Madison 1980 (American Institute of Physics, N.Y., 1981) p. 1196.

/3/ U.Amaldi et al., Rev. Nucl. Sci. 26 (1976) 385;
U.Idschok, Univ. Bonn, private communication.

/4/ A.Donnachie and G.Shaw, Electromagnetic Interactions of Hadrons, Vol. 2 (Plenum Press, N.Y., 1979) p. 169.

/5/ G.Veneziano, Nuovo Cim. A57 (1968) 190;
J.A.Shapiro, Phys. Rev. 179 (1969) 1345.

/6/ A.Cordier et al., Results of the DM1 Experiment at DCI: Observation of a ϕ' (1.65) vector meson, paper No. 143, submitted to this conference.

/7/ M.Binkley et al., J/ψ Photoproduction from 60 to 300 GeV/c, paper No. 58, submitted to this conference.

/8/ D.Aston et al., Photoproduction of ρ^0 and ω on Hydrogen at Photon Energies of 20 to 70 GeV, paper No. 137, submitted to this conference.

/9/ M.Atkinson et al., The Decay of the ρ' (1600) into $\pi^+\pi^-\pi^0\pi^0$, paper No. 211, submitted to this conference.

/10/ M.Atkinson et al., The Reaction $\gamma p \to \eta\pi^+\pi^- p$ for Energies of 20 - 70 GeV, paper No. 212, submitted to this conference.

/11/ M.Atkinson et al., The Reaction $\gamma p \to p\pi^+\pi^-\pi^0$ at Photon Energies of 20 - 70 GeV, paper No. 213, submitted to this conference.

/12/ M.Atkinson et al., Photoproduction of the $\omega\pi^0$ state in the Energy Range 20 - 70 GeV, paper No. 214, submitted to this conference.

/13/ P.M.Ivanov et al., Measurements of Charged Kaon Form Factor at the Energies below 1.4 GeV, paper No. 224, submitted to this conference.

/14/ R.M.Egloff et al.,Phys.Rev.Lett. 43 (1979) 657 and
Phys.Rev.Lett. 43 (1979) 1545.

/15/ D.Aston et al., Nucl.Phys. B 172 (1980) 1.

/16/ A.M.Breakstone et al., XX. Int.Conf. on High Energy Physics, Madison 1980 (American Institute of Physics, N.Y., 1981) p. 233.

/17/ J.Ballam et al., Phys.Rev. D7 (1973) 315o and D8 (1973) 1277.

/18/ P.Soeding, Phys.Lett. 19 (1966) 7o2.

/19/ T.H.Bauer et al, Rev. of Mod. Phys. 5o, No. 2, April 1978.

/2o/ K.Schilling et al., Nucl.Phys. B15 (197o) 39.

/21/ A.M.Eisner, Proc. 1979 Int. Symp. on Lepton and Photon Interactions at High Energies (FNAL-Pub., Batavia, 1979) p. 448.

/22/ D.S.Ayres et al., Phys.Rev. D15 (1977) 31o5.

/23/ D.Yennie, Phys.Rev.Lett. 34 (1975) 239.

/24/ D.W.S.Leith, Electromagnetic Interactions of Hadrons, Vol. 1 (Plenum Press, N.Y., 1979) p. 345.

/25/ A.Silverman, Proc. 1975 Int. Symp. on Lepton and Photon Interactions at High Energies (SLAC, Stanford, 1975) p. 355.

/26/ R.L.Anderson et al., Phys.Rev.Lett. 38 (1977) 263.

/27/ D.Sivers et al., Phys.Rev. D13 (1976) 1234.

/28/ K.Terasaki, Hiroshima University preprint 1981.

/29/ F.D.Gould and A.B.Rimmer, How large is $\sigma(\psi N)$?, paper No. 35, submitted to this conference.

/3o/ J.J.Aubert et al., Phys.Lett. 89B (198o) 267
A.R.Clark et al., Phys.Rev.Lett. 43 (1979) 187.

/31/ D.Aston et al., CERN /EP/ 81-13, Nucl.Phys. B189 (1981) 15.

/32/ M.S.Atiya et al., Phys.Rev.Lett. 43 (1979) 1691.

/33/ D.Aston et al., Phys.Lett. 92B (198o) 215.

/34/ Review of Particle Properties, Rev.Mod.Phys. 52 No. 2, Part II (April 198o)

/35/ C.D.Frogatt et al., Nucl.Phys. B129 (1977) 89.

/36/ F.Laplanche, Proc. 1977 Int. Symp. on Lepton and Photon Interactions at High Energies (DESY-Pub., Hamburg 1977) p. 189.

/37/ J.Perez y Jorba, Proc. 1978 Int. Conf. on High Energy Physics, Tokyo (Phys.Soc. of Japan, Tokyo, 1979)p. 277.

/38/ F.Cosme et al., Nucl.Phys. B152 (1979) 215.

/39/ U.Becker, Nucl.Phys. B151 (1979) 46.

/4o/ T.J.Killian et al., Phys.Rev. D21 (198o) 3oo5.

/41/ F.A.DiBianca et al., Phys.Rev. D23 (1981) 595.

/42/ A.Bramon and M.Greco, Lett. al Nuovo Cim. 3 (1972) 693;
G.Penso and T.N.Truong, Phys.Lett. 95B (198o) 143.

/43/ B.D'Almagne, Proc. XX. Int. Conf. on High Energy Physics, Madison, 198o (American Institute of Physics, N.Y., 1981) p. 221.

/44/ A.B.Clegg, Proc. XVIth Rencontre de Moriond (1981 Edition Frontières, Derux, 1981) in press.

/45/ J.Ballam et al., Phys.Rev.Lett.24 (197o) 1364;
G.Wolf, 1971 Int. Symp. on Electron and Photon Interactions (Lab. of Nuclear Studies, Cornell Univ., Cornell, 1972) p.189.

/46/ G.Höhler, TKP 76/1o, Karlsruhe (June 1976);
H.Joos, Acta Phys.Austriaca, Suppl.IV (1967) 32o.

/47/ V.Sidorov, Proc. 1979 Int. Symp. on Lepton and Photon Interactions at High Energies (FNAL-Pub., Batavia, 1979) p. 49o.

/48/ See for inst. J.P.Perez y Jorba and F.M.Renard, Phys.Reports 31C (1977) 1;
B.H.Wijk and G.Wolf, Electron-Positron Interactions, Springer Tracts in Mod. Phys., Vol. 86, Springer Verlag, Berlin, Heidelberg, New York 1979.

/49/ M.Spinetti, Proc. 1979 Int. Symp. on Lepton and Photon Interactions at High Energies (FNAL-Pub., Batavia, 1979) p. 5o6.

/5o/ F.M.Renard, Nuovo Cim. 64A (1979) 979.

/51/ H.Raszillier, Univ. Bonn, private communication.

/52/ S.U.Chung et al., Phys.Rev. D11 (1976) 2426.

/53/ D.P.Barber et al, Z.Phys. C4 (198o) 169;
D.Aston et al., Phys.Lett. 92B (198o) 211.

/54/ F.Richard, Proc. 1979 Int. Symp. on Lepton and Photon Interactions at High Energies (FNAL-Pub., Batavia, 1979) p.469;
D.Aston et al., Phys.Lett. 104B (1981) 231.

/55/ B.Esposito et al., Lettere al Nuovo Cim. 28 (198o) 195.

/56/ D.P.Barber et al., A Study of Elastic Photoproduction of Low Mass K^+K^- Pairs from Hydrogen in the Energy Range 2.8 - 4.8 GeV, submitted to Z.Phys.C.

1 The situation is in fact not fully clear. In a recent analysis of elastic photoproduction of ϕ between 2.8 and 4.8 GeV incident photon energy /56/ this difference is not observed. Assuming $0 \leq \eta_\phi \leq 0.2$ and $\sigma_{TOT}(\phi p) \approx 10$ mb (in agreement with naive quark model predictions), the value obtained is $\gamma_\phi^2/4\pi = 3.0 \pm 0.7$.

2 $\rho'(1600)$ could also decay through $(\rho\pi)\pi$ where the $\rho\pi$ system has isospin zero. Such a decay would contribute to the $\pi^+\pi^-\pi^0\pi^0$ final state (but not to $2\pi^+2\pi^-$).

3 Estimates based on the measured decay rate $A_1 \to \rho\pi$ (and the assumption that the same coupling holds at higher masses) yields typical values of

$\sigma(e^+e^- \to \rho^0 \to A_1\pi)$ of a few nb at a mass of 1.5 GeV /51/.

4 In previous analyses this assumption was always applied because of poor statistics /53/.

Discussion

M. Roos, Helsinki: The Cosme data you showed with the $\pi^+\pi^-\pi^o$ peak was taken with a detector without magnetic field. Also they cannot distinguish $\pi^+\pi^-\pi^o$ from the $\pi^+\pi^-(\gamma)$ background. The DM1 experiment has an upper limit to the $\pi^+\pi^-\pi^o$ cross section which disagrees with Cosme, so there is a background problem. In consequence I don't think one should take the narrow Cosme peak very seriously.

E. Paul: Yes. However, one must then answer the question, how well one understands in the experiment with the DM1 spectrometer the separation of the $\pi^+\pi^-\pi^o$ channel from $e^+e^- \to$ two charged particles (eventually plus radiative photons). I remind you that secondary photons (from π^0 decay) are not detected here.

B. Delcourt, Paris: About the $e^+e^- \to \pi^+\pi^-\pi^0$ peak found by Cosme et al., the problem is that it suffers from statistics: it is only a three standard deviation peak. DM1 did not publish anything on this subject because we cannot separate $e^+e^- \to \rho^0\pi^0$ from $e^+e^- \to e^+e^-\gamma \to \rho^0\gamma$. The only thing we know is that it has not a large cross section.

B. Stella, DESY: It is not completely correct to compare DM1 results on $e^+e^- \to 2\pi^+2\pi^-$ (which are much higher than ADONE and VEPP 2 results in the low energy region) with available data on $e^+e^- \to \pi^+\pi^-2\pi^0$. In fact the DM1 experiment has a good resolution, exclusive, small solid angle and has no shower detection. The $\gamma\gamma 2$ measurement of $\pi^+\pi^-2\pi^0$, though with large solid angle, good resolution and efficiency for showers, is strongly correlated to the $2\pi^+2\pi^-$ result. Only the $4\pi(2\pi^+2\pi^-+\pi^+\pi^-2\pi^0)$ cross section seems to be in agreement in all experiments (at Frascati, Orsay and Novosibirsk). Then, if the $2\pi^+2\pi^-$ cross section would have to be higher than found in previous (but DM1) measurements, the $\pi^+\pi^-2\pi^0$ should consequently be lower, since the total 4π cross sections look well-established. This would leave even less room for a $\rho'(1250)$ and for a $\rho'(1600) \to \rho\varepsilon$ contribution, but also would not fit with the $\rho'(1600) \to A_1\pi$ hypothesis (since the $2\pi^+2\pi^-$ channel would be a factor ~ 2 larger than $\pi^+\pi^-2\pi^0$).